Recent Progress in Two-dimensional Systems

Institute for Research in
Fundamental Sciences, Tehran
October 2014

Observing Wigner Crystals in Double Sheet Graphene Systems in Quantum Hall Regime

Bahman Roostaei

IUPUI
DEPARTMENT OF PHYSICS
SCHOOL OF SCIENCE
A Purdue University School
Indianapolis

Double Sheet Graphene

Equivalent properties of Dirac Electrons and Dirac Holes:

-Symmetric Bands

- -Adjustable polarity of carriers
- -possibility of fabrication not limited to Graphene.
- - suppression of interlayer tunneling even at small separations: Larger parts of phase space.

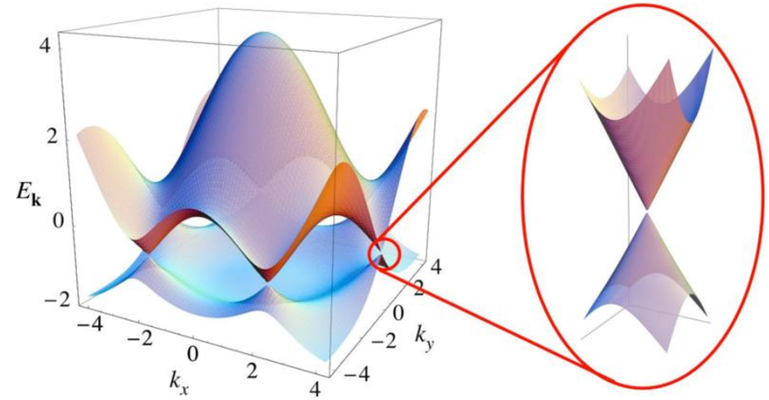

Castron Neto et. Al. 2009

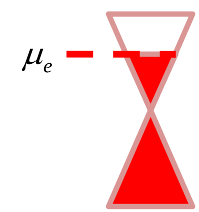

We assume two valley polarized sheets under strong perpendicular magnetic field.

$$\ell_B = \sqrt{\hbar / eB}$$

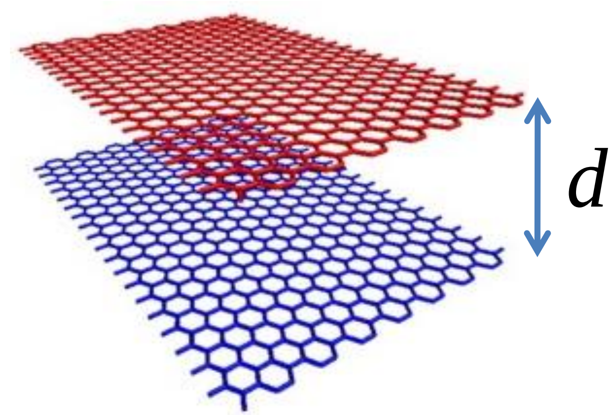

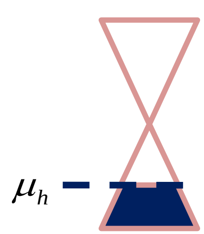

Comparison:

$$d / \ell_B < 1$$

$$d / \ell_B \approx 1$$

$$d / \ell_B > 1$$

Story of Wigner Crystal

Electron gas in two dimensions:

Quantum Well (B=0):

Kinetic Energy per particle $\propto n^2$
Coulomb Energy per particle $\propto n^{3/2}$

Graphene (B=0):

Kinetic Energy per particle $\propto n^{3/2}$
Coulomb Energy per particle $\propto n^{3/2}$

Under Strong Magnetic Field:

> Confined to Landau Levels

> Kinetic Energy is frozen.

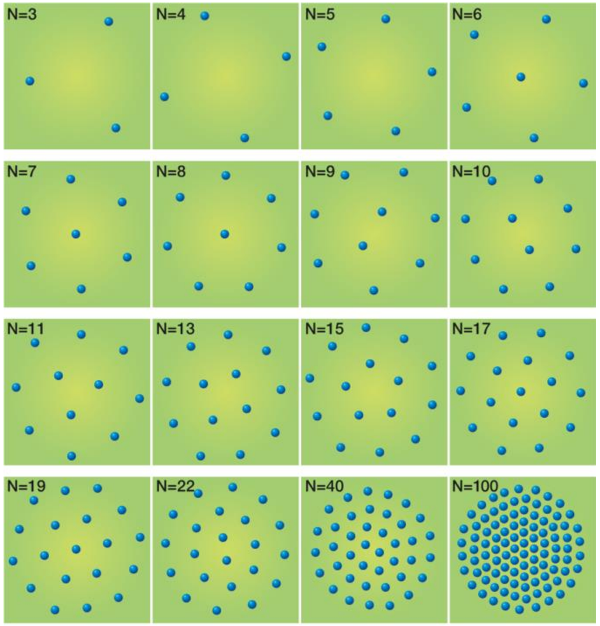

Ground state configurations for N=3 to 100

Physics ***2****, 4 (2009)*

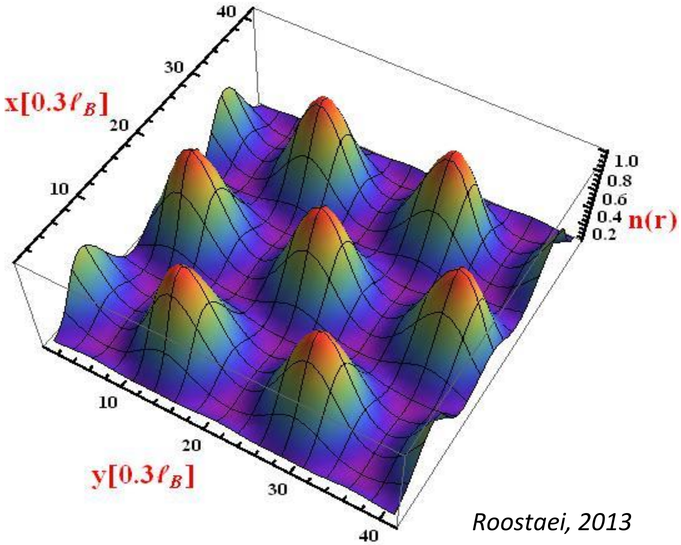

Roostaei, 2013

Questions and Motivations

➢ Using barrier layers such as hBN.

➢ It is possible to fabricate closely spaced double sheet Graphene structures.

$d/\ell < 1$

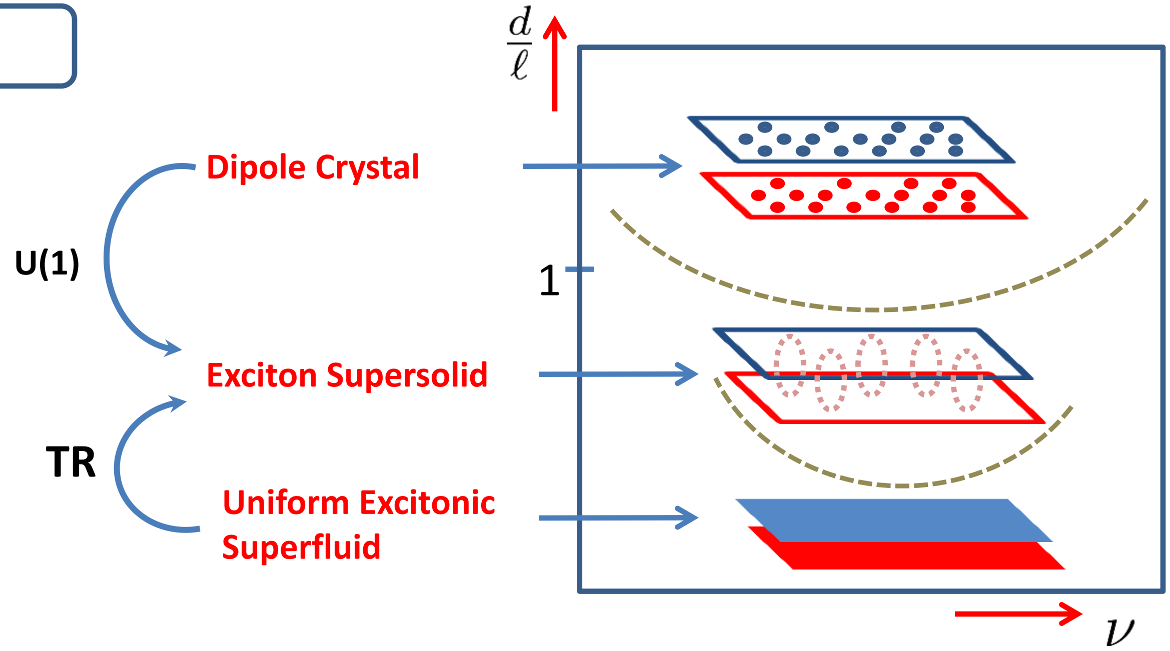

➢ At these small separations excitons may form :

➢Does U(1) Symmetry break ?

❑ Does BEC happen?

➢Does Wigner Crystal of Excitons form ?

❑Does Translational Symmetry Break ?

➢Do both of these symmetries break at the same boundary ? No ➡ Supersolid???

Where do these symmetries break ?

Adjacent Electron-Hole Sheets

Method of calculation : Hartree-Fock
Numerical Self Consistent Iteration:

$$\rho_N^{\sigma\sigma'}(\mathbf{r}) = \left\langle \hat{\psi}_{N\sigma}^{\dagger}(\mathbf{r})\hat{\psi}_{N\sigma'}(\mathbf{r}) \right\rangle$$

$$\begin{aligned} H_{HF} &= \frac{N_\phi e^2}{\epsilon\ell}\sum_{\sigma,\mathbf{Q}}\left[\frac{E_N}{e^2/\epsilon\ell}\delta_{\mathbf{Q},0} + H_N^{\sigma\sigma}(\mathbf{Q}) - X_N^{\sigma\sigma}(\mathbf{Q})\right]\hat{\rho}_N^{\sigma\sigma}(\mathbf{Q}) \\ &- \frac{N_\phi e^2}{\epsilon\ell}\sum_{\sigma,\mathbf{Q}}\left[H_N^{\bar{\sigma}\bar{\sigma}}(\mathbf{Q})\hat{\rho}_N^{\sigma\sigma}(\mathbf{Q}) + X_N^{\sigma\bar{\sigma}}(\mathbf{Q})\hat{\rho}_N^{\bar{\sigma}\sigma}(\mathbf{Q})\right] \end{aligned}$$

$$\begin{aligned} \delta_{\mathbf{Q},0} I &= \begin{bmatrix} i\omega+\mu & 0 \\ 0 & i\omega-\mu \end{bmatrix} G_N(\mathbf{Q}, i\omega) \\ &- \sum_{\mathbf{Q}'}\begin{bmatrix} \Sigma_{ee}(\mathbf{Q}-\mathbf{Q}') & \Sigma_{eh}(\mathbf{Q}-\mathbf{Q}') \\ \Sigma_{he}(\mathbf{Q}-\mathbf{Q}') & -\Sigma_{hh}(\mathbf{Q}-\mathbf{Q}') \end{bmatrix} e^{i\mathbf{Q}\times\mathbf{Q}'\ell^2/2} G_N(\mathbf{Q}', i\omega) \end{aligned}$$

$$\begin{aligned} \Sigma_{ee}(\mathbf{Q}) &= \left[H_N^{ee}(\mathbf{Q}) - X_N^{ee}(\mathbf{Q})\right]\rho_N^{ee}(-\mathbf{Q}) \\ &- H_N^{eh}(\mathbf{Q})\rho_N^{hh}(-\mathbf{Q}) \\ \Sigma_{eh}(\mathbf{Q}) &= -X_N^{eh}(\mathbf{Q})\rho_N^{eh}(-\mathbf{Q}) \end{aligned}$$

States we consider: $\rho_{ee}(\mathbf{Q}) = \rho_{hh}(\mathbf{Q})$

$$\rho_{eh}(\mathbf{Q}) \begin{cases} =0 \\ \neq 0 \end{cases}$$

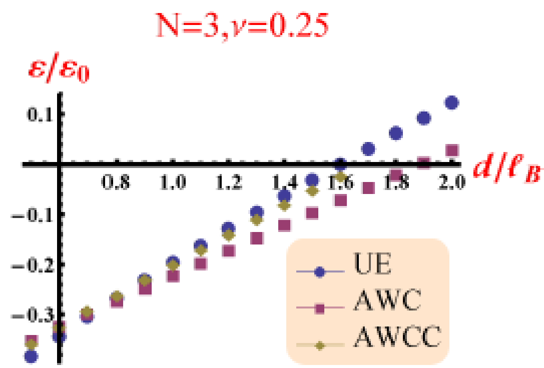

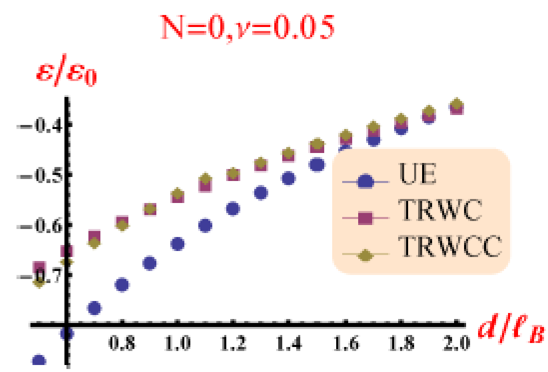

Adjacent Electron-Hole Sheets

Anisotropic Crystals are more abundant at higher LL.

Uniform Excitonic States Exist at smaller separations.

No Exciton Crystal Ground State !

$$\mathbf{a}_1 = \{a, b/2\} \text{ and } \mathbf{a}_2 = \{0, b\}$$

$$a = \sqrt{2\pi/\nu\gamma}$$

$$\gamma = b/a$$

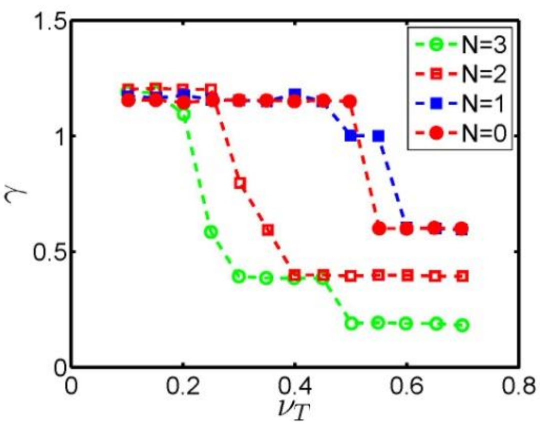

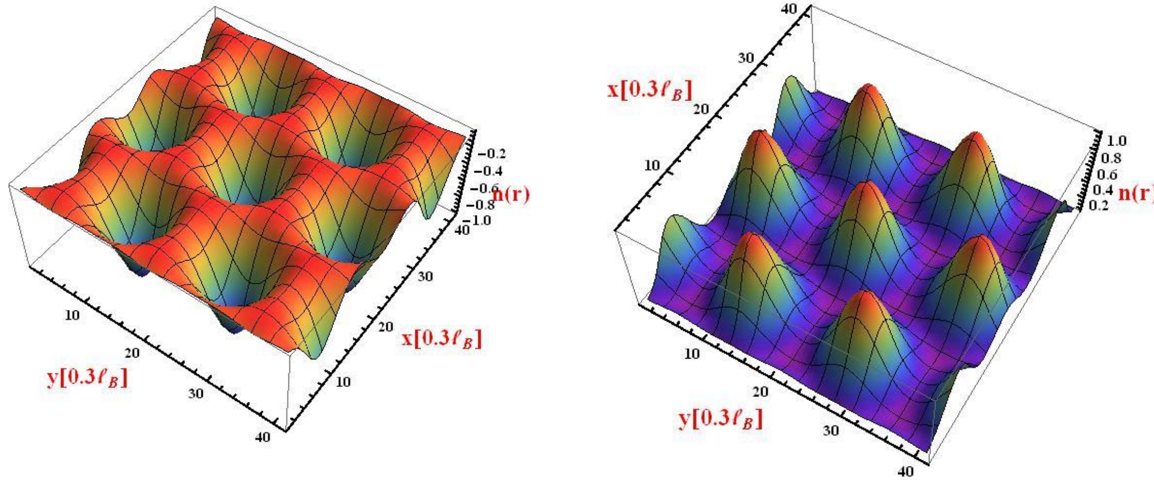

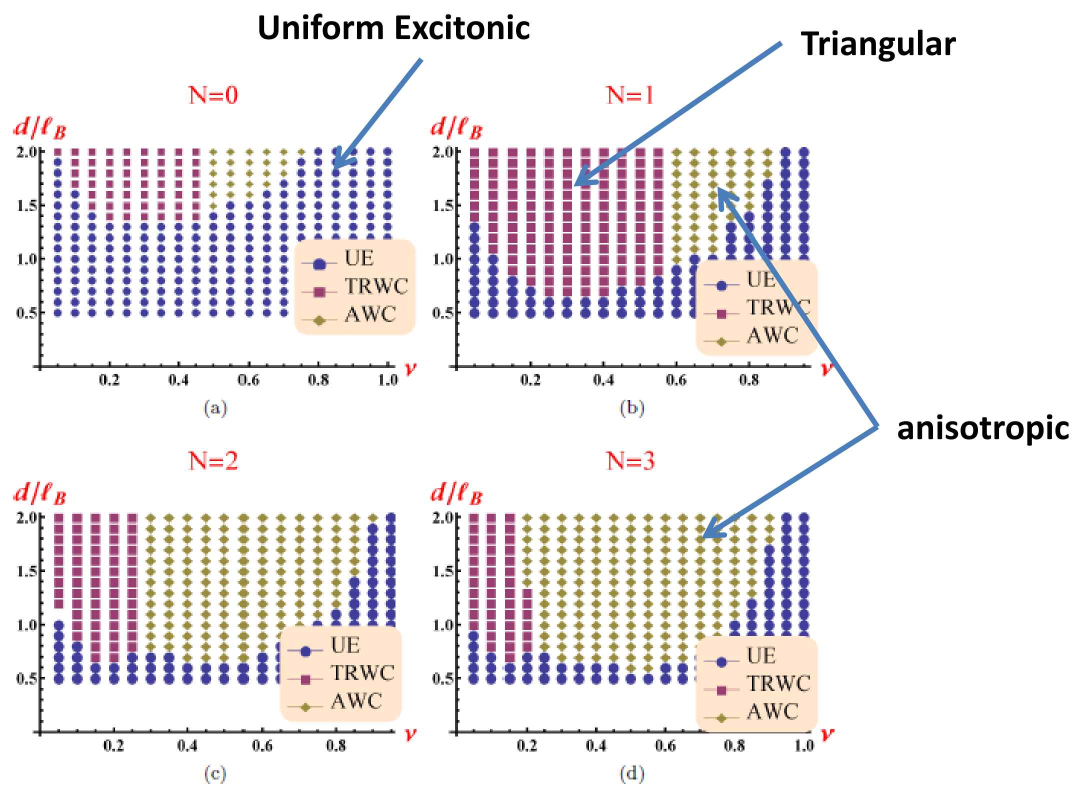

Detection of Dipole Wigner Crystals In Graphene

Capacitance Measurement:

Metal electrode close to the layer

Adjacent Electron – Hole layers :
Image charges.

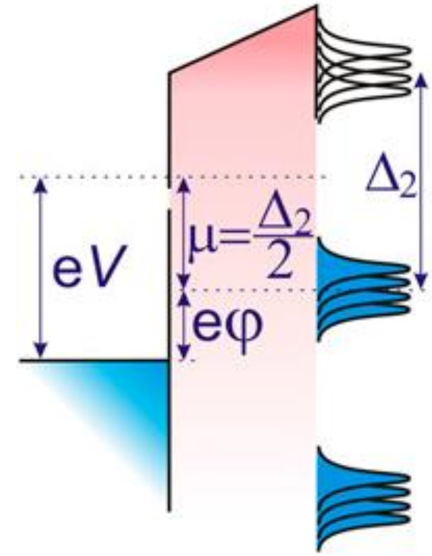

G. L. Yu, et.al. , PNAS 2013

$$C_g = \epsilon / d \qquad C = \left(C_g^{-1} + \frac{1}{e^2} \frac{d\mu}{dn} \right)^{-1}$$

$$d^* = d + d_Q$$

$$d_Q = \frac{\ell_B}{4} \frac{d^2}{d\nu^2} \left[\frac{\nu E(\nu)}{e^2 / \epsilon \ell} \right] \geq -d$$

Effect of Image Charges is to renormalize the capacitance:

Excitonic Condensate $\quad d < \ell_B$

Interactions $\quad d \approx \ell_B$

Photoluminescence:
Electron – Hole Recombination

STM : LDOS

Detection of Dipole Wigner Crystals In Graphene

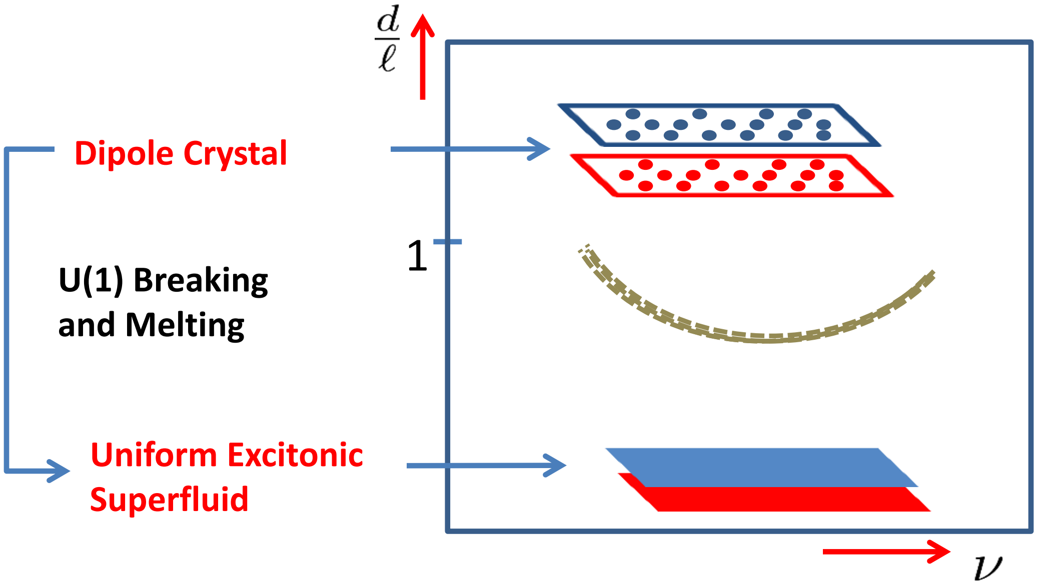

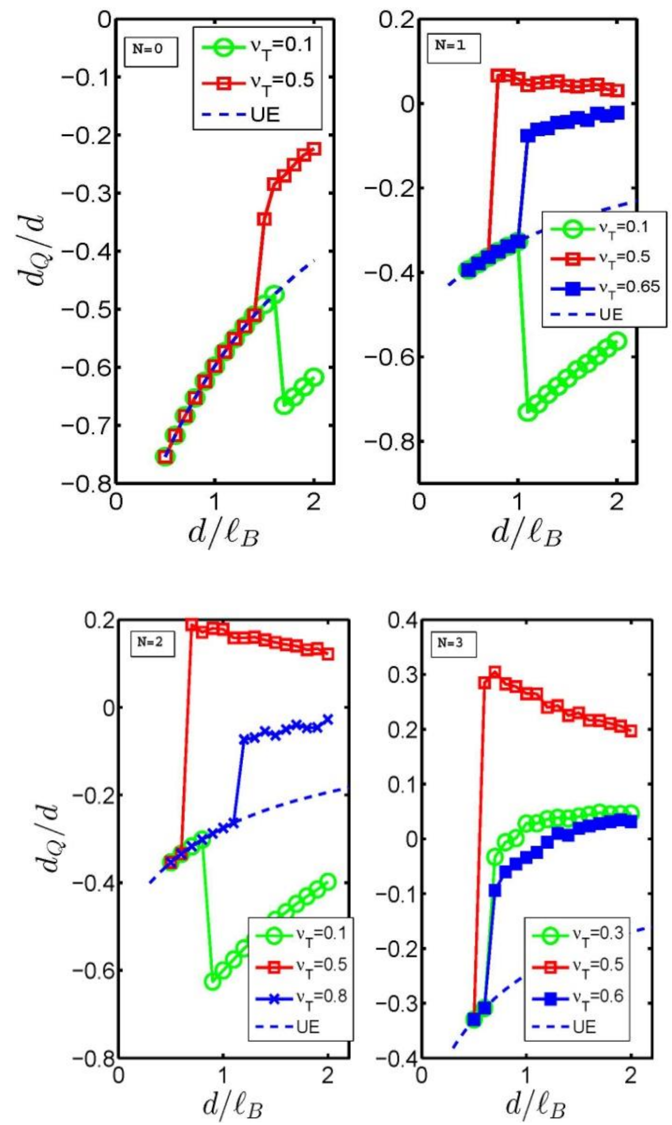

Extra effects

Interestingly peaks can be observed at □ □ 0.3 !

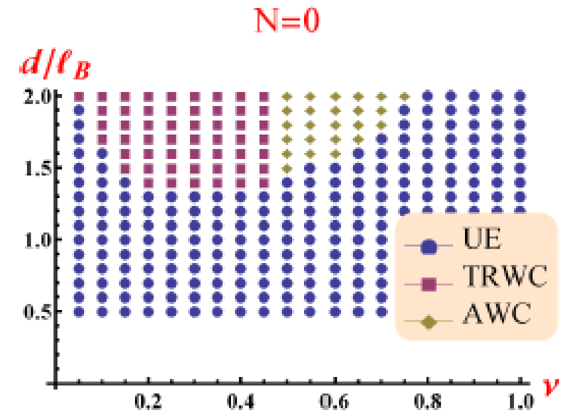

Dipole crystal state

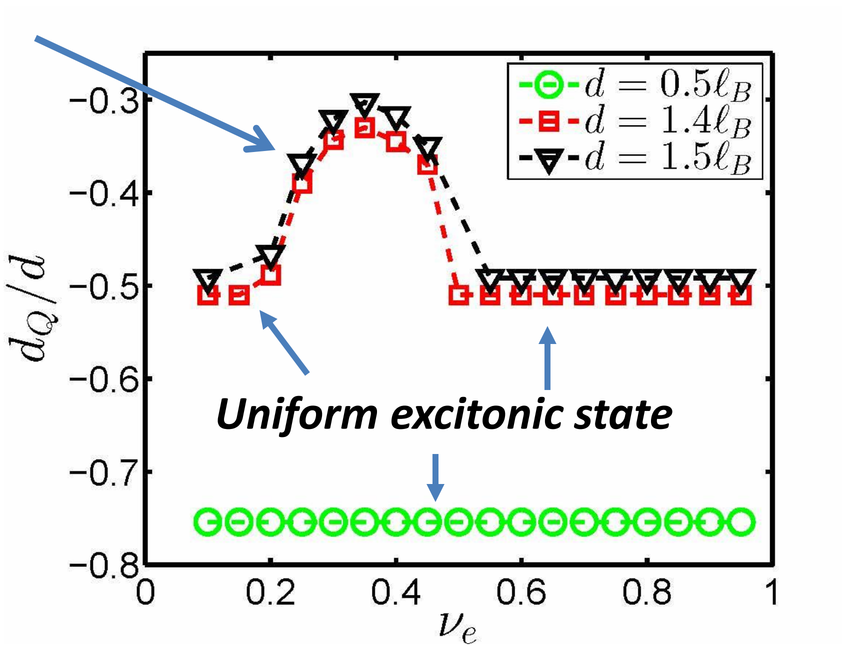

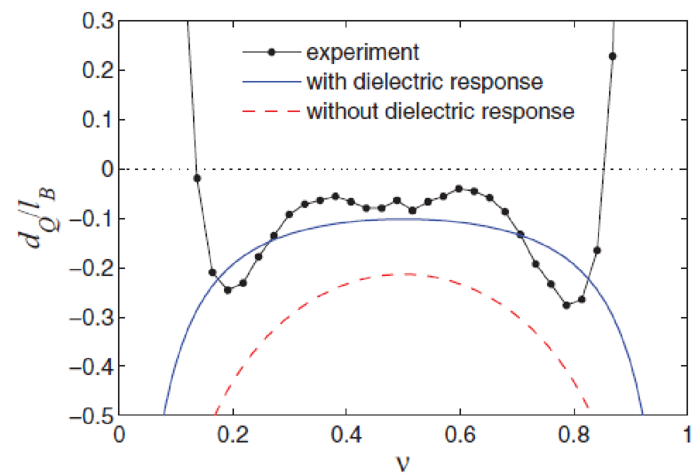

B. Skinner , et. Al. 2013

Photoluminescence Spectrum

Optically pumped electron-hole system is another type of e-h systems.

Due to highly resistive barriers (hBN) e-h recombination is delayed.

The system has enough time to find its ground state.

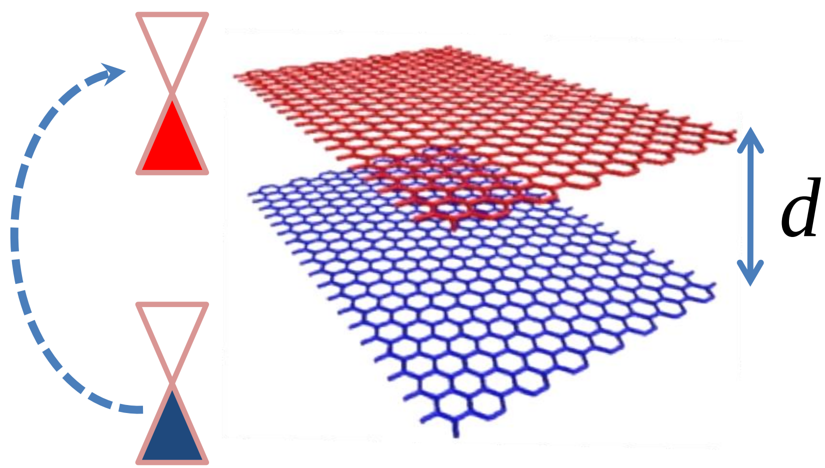

The recombination spectrum carries information about the state of the system.

The spectrum changes as filling factor and interlayer separation changes.

$$P(\omega) = \frac{1}{Z}\sum_{n,m} e^{-\beta E_n} \left|\left\langle n; N-1 \middle| \hat{U} \middle| m; N \right\rangle\right|^2 \times$$
$$\times\, \delta(\omega + E_n - E_m)$$

$$\hat{U}(\tau) = \mu_0 \int d^2\mathbf{r}\hat{\psi}_e(\mathbf{r},\tau)\hat{\psi}_h(\mathbf{r},\tau)$$

$$R(\tau) = -T_\tau \left\langle \hat{U}(\tau)\hat{U}(0) \right\rangle$$

Information about the interactions and ground state wavefunction

$$R(i\omega_n) \approx \mu_0^2 {\sum_{\lambda\lambda'}}' \sum_{\mathbf{Q}} \frac{W_e^{\lambda}(\mathbf{Q})W_h^{\lambda'}(-\mathbf{Q})}{i\omega_n - \omega_\lambda - \omega_{\lambda'}}$$

Story of Photoluminescence of Wigner Crystal - 1

In traditional quantum wells, holes bound to dopant atoms may recombine with electrons in quantum well.

Band structure of an electron interacting with a Wigner crystal with filling factor p/q : p bands occupied out of q bands.

It is therefore expected that there are p peaks observable in PL spectrum.

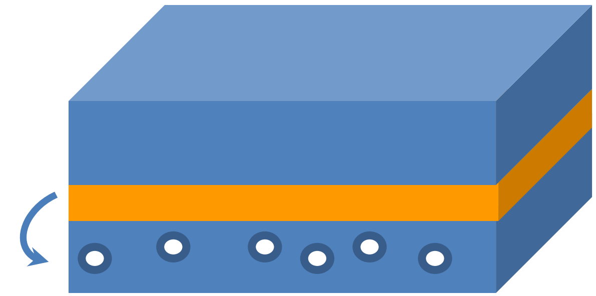

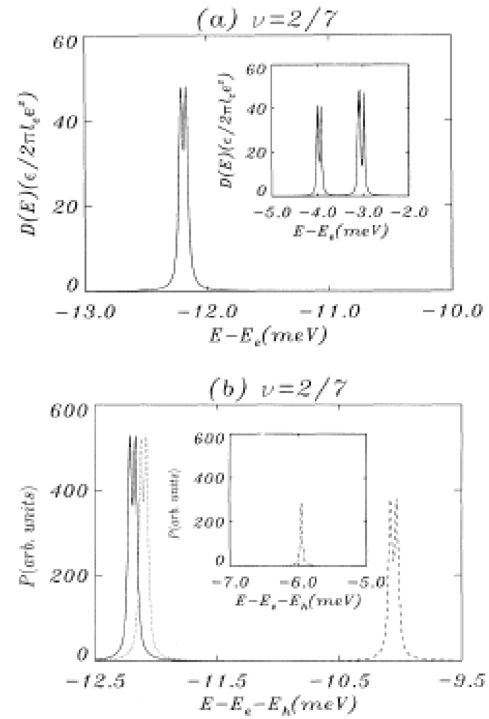

FIG. 2. Electron density of states and PL spectrum for perfect WC with no electron-hole interaction for $\nu = 2/7$. (a) Electron DOS below chemical potential at zero temperature (inset: DOS above chemical potential), where $E_c = \frac{1}{2}\omega_c$; (b) PL spectrum at different temperatures: $T = 0.0045T_{\mathrm{melt}}$ (solid), $T = 0.45T_{\mathrm{melt}}$ (dotted), $T = 0.9T_{\mathrm{melt}}$ (dashed), and $T = 1.12T_{\mathrm{melt}}$ (inset: dash-dotted).

D. Z. Liu, H. A. Fertig, S. Das Sarma, PRB 1993.

Story of Photoluminescence of Wigner Crystal - 2

However : Interaction of holes with the crystal results in the distortion of the crystal hence wiping out the PL structure.

Obviously disorder distribution of holes creates another obstacle in detection of Wigner crystal.

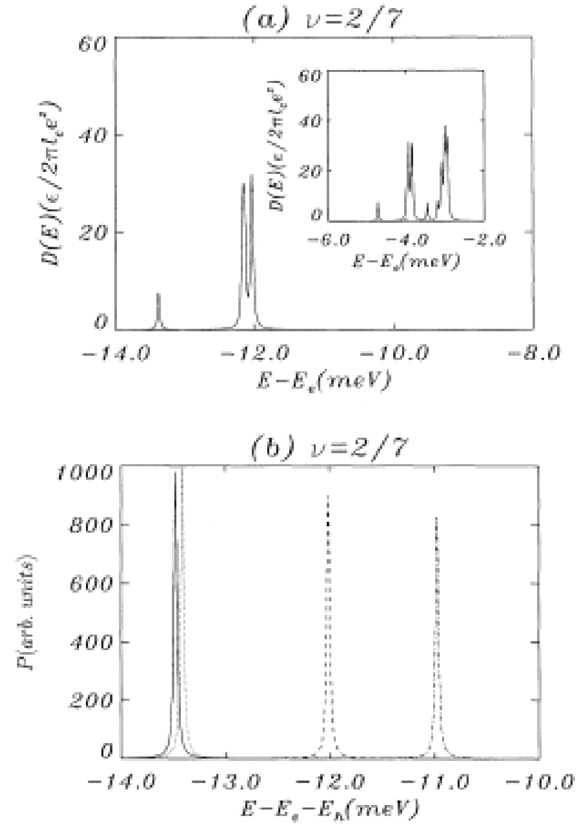

FIG. 3. Electron density of states and PL spectrum for WC in the presence of unscreened interaction between electrons and localized holes for $\nu = 2/7$. (a) Electron DOS below chemical potential at zero temperature (inset: DOS above chemical potential); (b) PL spectrum at different temperatures: $T = 0.0045T_{\rm melt}$ (solid), $T = 0.45T_{\rm melt}$ (dotted), $T = 0.9T_{\rm melt}$ (dashed), and $T = 1.01T_{\rm melt}$ (dash-dotted).

D. Z. Liu, H. A. Fertig, S. Das Sarma, PRB 1993.

Photoluminescence of Dipole Wigner Crystals

Dipole Wigner crystals are made out of slightly different carrier type :their recombination spectrum is free of external effects !

Interestingly a fully interacting electron-hole system shows the same PL spectrum!

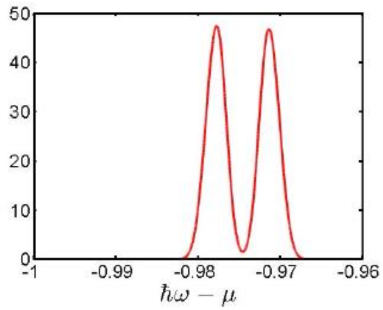

FIG. 1. Mean field photoluminescence spectrum of triangular Wigner crystal of dipoles at balanced electron-hole double monolayer Graphene each having filling factor $\nu = 2/7$. The layer separation here is chosen to be $d = 1.5\ell_B$ and the energies are in units of $e^2/\epsilon\ell_B$.

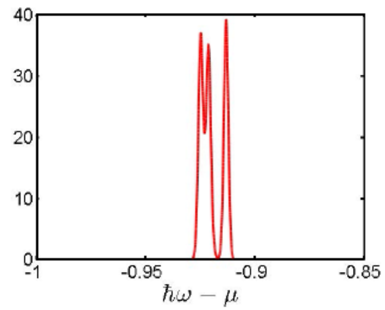

FIG. 2. Mean field photoluminescence spectrum of triangular Wigner crystal of dipoles at balanced electron-hole double monolayer Graphene each having filling factor $\nu = 3/7$. The layer separation here is chosen to be $d = 1.5\ell_B$ and the energies are in units of $e^2/\epsilon\ell_B$.

Roostaei, unpublished

Photoluminescence of Dipole Wigner Crystals : *Control knobs*

By changing the filling factor the PL spectrum evolves in a particular way.

The peak positions also evolve as a function of interlayer separation.

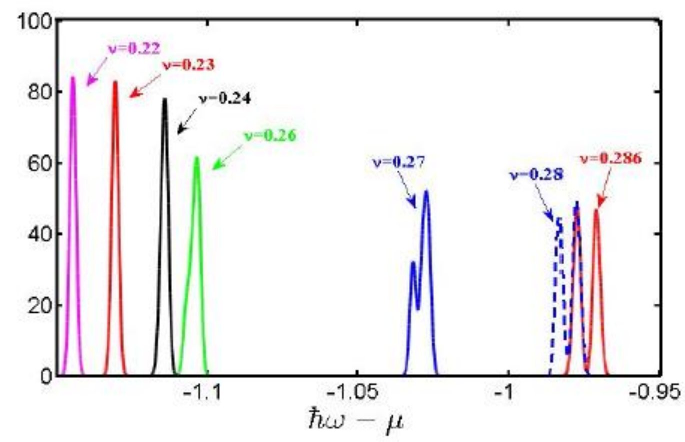

FIG. 3. Mean field evolution of photoluminescence spectrum of triangular Wigner crystal of dipoles at balanced electron-hole double monolayer Graphene as the filling factor changes. The layer separation here is chosen to be $d = 1.5\ell_B$ and the energies are in units of $e^2/\epsilon\ell_B$.

Roostaei, unpublished

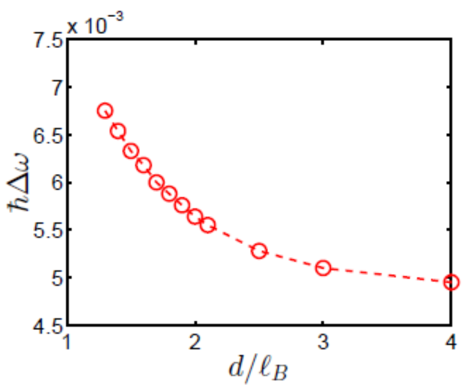

FIG. 4. Separation between the two peaks (in units of $e^2/\epsilon\ell_B$) in photoluminescence spectrum of triangular Wigner crystal of dipoles at balanced electron-hole double monolayer Graphene at filling factor $\nu = 2/7$ as a function of layer separation.

Photoluminescence of Exciton Wigner Crystals?

PL evolution can signal the change of phase.

Excitonic crystals have even richer PL spectrum.

Parallel magnetic field couples with the phase of the excitonic condensate.

Therefore in-plane magneric field may shift the recombination spectrum.

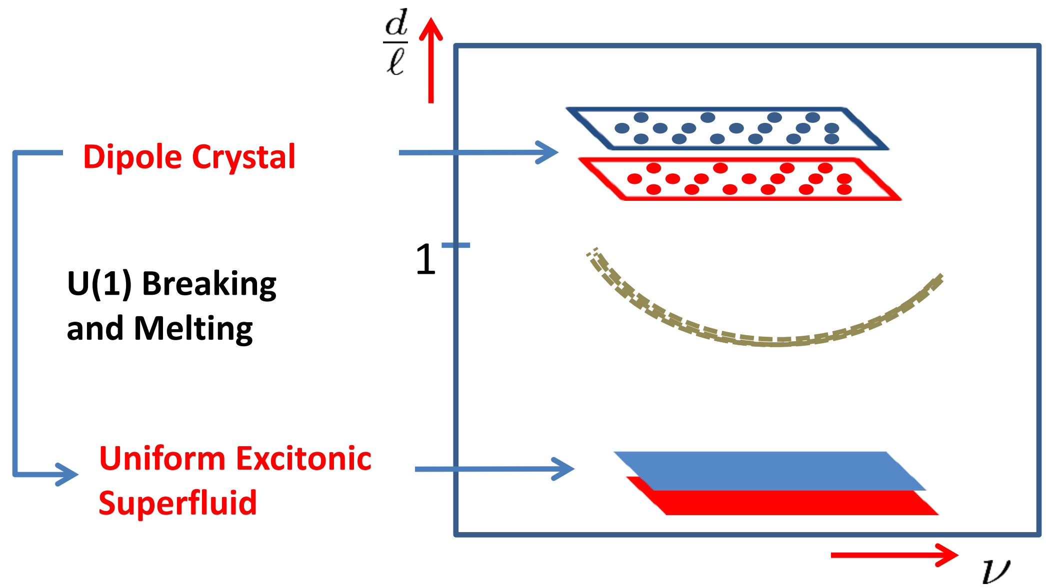

Another signature to tell apart excitonic crystal from dipole crystal.

Summary

It is possible to model capacitance by electron-hole double layer system.

Interactions greatly renormalize the capacitance in the Wigner Crystal Regime:

There is a jump in transition to excitonic condensate.

Anisotropic states have smaller capacitance.

The photoluminescence of dipole and exciton Wigner crystal can be observed, in principle.

Photoluminescence of dipole and exciton crystals can be manipulated by external control knobs such as density, magnetic field and tilt of the sample.

Existence of a supersolid of excitons is still an important open question.

The behavior of capacitance of the Wigner crystal as a function of filling factor is still not very well understood.

The phases of excitonic system in presence of disorder and its capacitance behavior is still not explored.

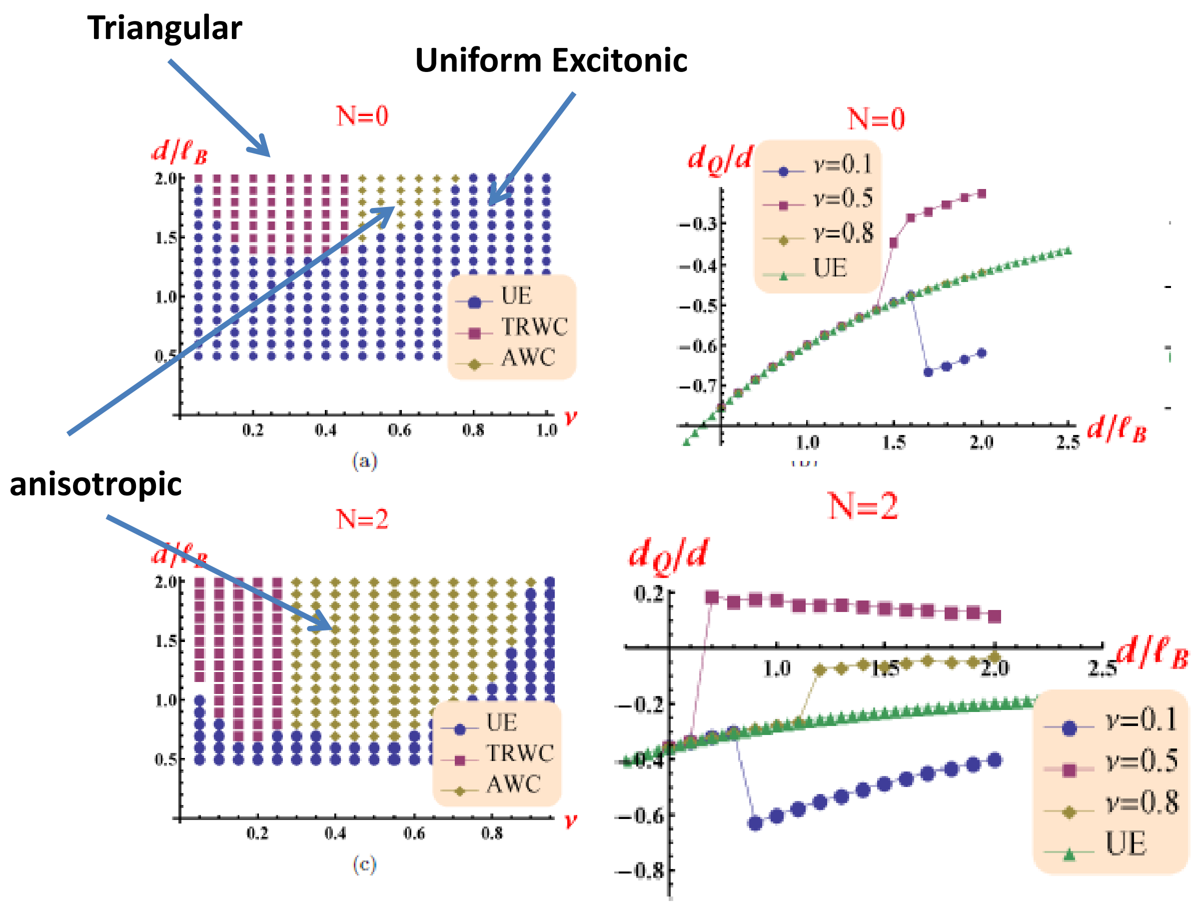

Triangular
Uniform Excitonic
anisotropic
N=0
N=2
UE
TRWC
AWC
ν=0.1
ν=0.5
ν=0.8
UE
(a)
(c)

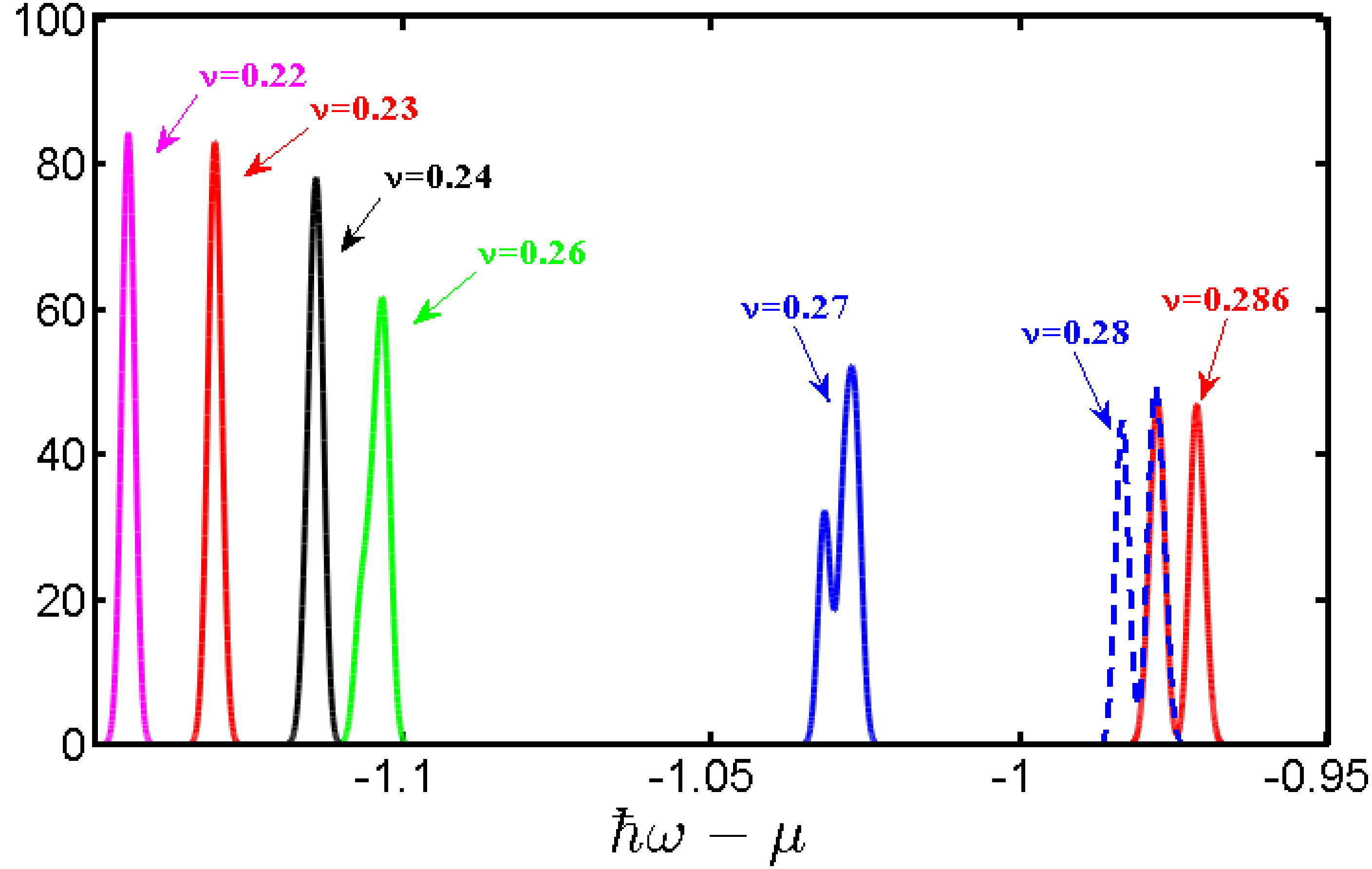

100
80
60
40
20
0
-1.1
-1.05
-1
-0.95
$\hbar\omega - \mu$
ν=0.22
ν=0.23
ν=0.24
ν=0.26
ν=0.27
ν=0.28
ν=0.286